공학석사학위논문

방사형 익스팬더 VGN 노즐의 멀티-캐비티 팁 누설 유동 저감 효과

Effect of multi-cavity tip on tip leakage flow in variable geometry nozzle of radial expander

2022년 8월

서울대학교 대학원

기계공학부

송 자 연

방사형 익스팬더 VGN 노즐의 멀티-캐비티 팁 누설 유동 저감 효과

Effect of multi-cavity tip on tip leakage flow in variable geometry nozzle of radial expander

지도교수 송 성 진

이 논문을 공학석사 학위논문으로 제출함

2022년 4월

서울대학교 대학원

기계공학부

송 자 연

송 자 연의 공학석사 학위논문을 인준함

2022년 6월

위 원 장 : 김 호 영 (인)

부위원장 : 송 성 진 (인)

위 원 : 황 원 태 (인)

Abstract

Effect of Multi-Cavity Tip on Tip Leakage Flow in Variable Geometry Nozzle of radial expander

Jayeon Song
Department of Mechanical Engineering
The Graduate School
Seoul National University

A numerical research has been conducted for a radial expander with Variable Geometric Nozzle (VGN) to analyze its tip leakage flow rate using CFD.

The tip discharge coefficients are calculated for the flat tips, the squealer tips, and the cavity tips to choose a design factor that has the smallest discharge coefficient. The cavity tip is selected and applied to the VGN of the radial expander as a design factor to reduce its tip leakage flow rate.

The tip leakage flow rates along the pressure side, the suction side, and the leading edge side are numerically calculated compared to the flat tip. Their flow mechanism is investigated depending on the streamwise location.

VGN blade with the cavity tip applied had little labyrinth seal effect due to the blade thickness and non-rotation characteristic of the nozzle blade, and there was little change in the tip leakage flow rate. Thus, the multi-cavity tip idea, a new shape to complement the thick blade thickness, was devised and applied to VGN. VGN blade with the multi-cavity tip had a partially reduced leakage flow rate

on the pressure side compared to the flat tip, and the size of the leakage flow vortex was increased and reduced the bulk flow angle of the VGN outlet.

Numerical calculations indicated that applying the multi-cavity tip to the VGN blade increased the aerodynamic efficiency by 1.25%p due to the reduction of the leakage flow rate at the pressure side and reduced flow angle of the VGN outlet.

Keyword : Radial expander, Variable Geometry Nozzle, Tip leakage flow, Cavity tip, Multi-cavity tip

Student Number : 2020-20449

Table of Contents

List of Tables

List of Figures

Chapter 1. Introduction

1.1 Research Background

A radial expander is a turbo machine that expands gas to obtain energy, used for various purposes in industrial sites such as recovering electrical energy from a natural gas transportation.

To get a wide operating range, Variable Geometric Nozzle (VGN) is particularly preferred because the mass flow rate can be controlled by adjusting the angle of the nozzle and eventually aiming desired velocity at the nozzle outlet. These advantages of VGN, however, essentially involve a gap between the nozzle blade and the casing.

1.2 Thesis Aims

In previous research, changing the tip shape of the radial turbine VGN does not exist. The previous research on the cavity tip have been done only in the axial turbine rotor not in the radial turbine VGN, and analysis on the complex shaped tip structure for the radial turbine VGN has not abundantly been conducted. Therefore, to reduce the leakage flow loss of the radial expander, applying the cavity tip to VGN and analyzing its internal flow are further required.

Chapter 2. Literature Review

2.1 Radial expander

The expander is a type of turbine that obtains energy by expanding gas. It is used for propulsion and energy generation in aviation and industrial sites such as jet engine turbines and most power plants. The expander is largely classified into an axial expander and a radial expander. Unlike an axial expander, in a radial expander, the inlet flow is bent at right angles to the rotor. The radial expander has the advantages of high performance, wide operating range, and small size compared to the axial flow expander, so it is mainly used in special situations that require high power generation in a narrow space.

2.2 Tip leakage flow in turbine

The shroud of the turbine rotor prevents gas leakage and protects the blades. Inevitably there is a tip gap between the shroud (the casing in the case of an unshrouded turbine) and the rotating blade. The tip clearance of unshrouded axial turbine blades with the casing is typically 1−2% of the blade span, and this tip clearance creates

leakage flow and is a major cause of reduced turbine stage efficiency.

Leakage flow between the blade tips is caused by the pressure difference between the pressure and suction side of the blades, as the fluid flows from the relatively high pressure side to the low suction side.

The VGN of the radial turbine controls the flow rate as shown in Figure 2.1, and there is a tip clearance between the nozzle and the casing from this structure.

Figure 2.1 Flow control through nozzle angle adjustment using VGN [1]

Liu et al. [2] was numerically shown that the leakage flow through this gap causes aerodynamic loss generated by the mixing at the rear end of the VGN as shown in Figure 2.2. This unsteady simulation also showed the tip leakage flow of the VGN causes the change in the nozzle exit flow angle, and the effect of the gap flow leads to the shock generated. This aerodynamic loss is reported to

have an effect on overall expander performance.

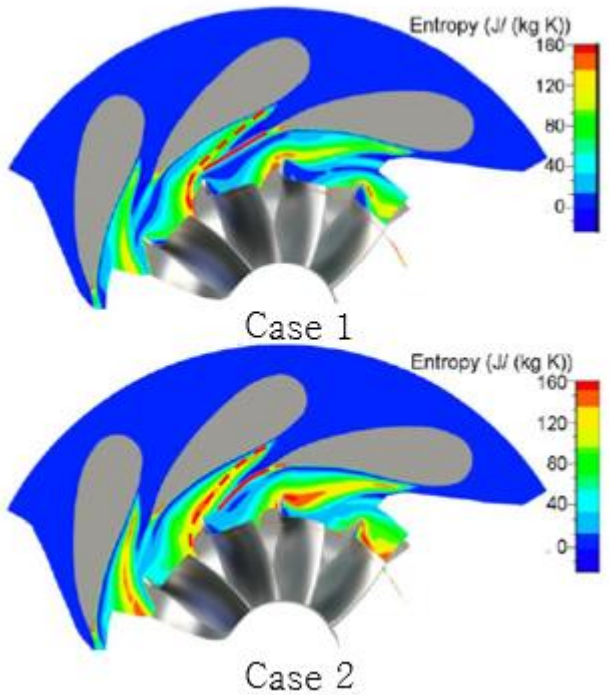

Figure 2.2 Entropy distribution countour in the shroud plane of VGN [2]

2.3 Tip Leakage Flow Reduction

2.3.1 Mechanism of Tip Leakage Flow

To improve aerodynamic performance of turbomachines, the leakage flow through their tip clearance is analyzed in various way. The flow pattern inside the tip gap is determined by the ratio of the blade thickness(t) to the tip gap width(τ) as shown in Figure 2.3. In

the case of a relatively thick blade flow reattachment occurs, but in the case of a thin blade the flow exits to the suction side without reattachment [3]. The flow entering the tip gap has a minimum cross-sectional area at 1.5τ and it gradually expands and mixes, suggesting that Sjolander and Cao [4] and Heyes and Hodson [5] show that the flow reattachment occurs at the point of 2.4τ and at 6τ.

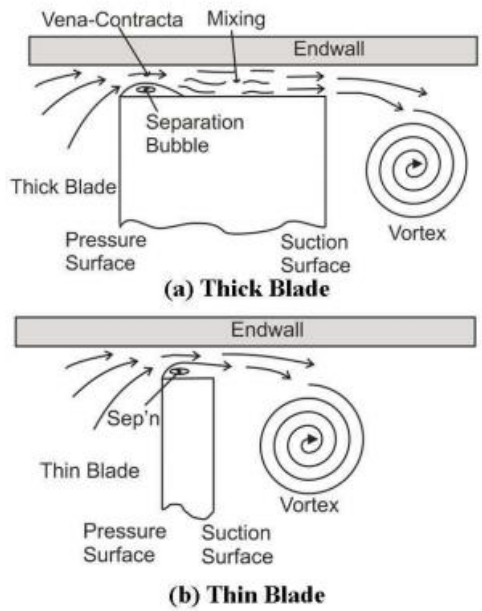

Figure 2.3 Tip leakage flow in unshrouded blades [3]

Denton and Cumpsty [6] found that the flow over the blade tip is not turned along the blade reducing the flow rate of the main flow and thus it reduces the overall blade loading. The tip leakage flow generates entropy by viscous force inside the tip gap and it mixes with the main flow after passing through the tip gap, causing

aerodynamic loss.

2.3.2 Axial Turbine Tip Leakage Flow Reduction

Since this leakage flow is inevitably generated at the turbine rotor, many studies for an axial turbine have been preceded on a method to reduce the leakage flow. Methods including applying the squealer tip and the cavity tip is widely used to the rotor blade tip of the axial turbine.

Squealer Tip

The squealer tip refers to a tip shape in which the squealer protrudes from one of the pressure side or the suction side. In the case of the pressure side squealer, the tip leakage flow loss may increase with blade thickness in the axial turbine. Thus, the suction side squealer is generally used which has a better loss reduction effect. It shows less loss reduction than the cavity tip (5~8%), but it is widely used because it is easy to machine [7].

Cavity Tip

The cavity tip refers to a tip shape with squealer tips along the blade profile on both the pressure side and the suction side. According to P. J. Newton [8], confinement of the vorticity within the cavity reduces the leakage flow rate and thus reduces the aerodynamic loss from the leakage flow by 10% for the axial

turbine. As flow contraction occurs above the squealer tip, the leakage flow rate decreases compared to the flat tip with an equal pressure drop from the pressure side to the suction side. Therefore, the cavity tip is more effective than the squealer tip because the vena contracta occurs twice on both the pressure side and the suction side.

Schabowski et al. [9] found that the squealer must be thin enough to prevent reattachment of the separated flow at the tip gap. Reattachment at the tip gap results in a greater pressure drop in the vena contracta and increases the tip clearance loss.

Zhou [10] showed that the cavity tip forms a vortex within the cavity, and the tip leakage flow decelerates as its mixing process occur with the existing flow in the gap. Thus, the cavity tip forms the leakage vortex which has lower stagnation pressure coefficient within the vortex core than that of the flat tip. In the case of rotation with end-wall motion, the moving end-wall applies tangential viscous force to the tip gap flow so that the vortex position changes in the tangential direction, and the cavity effect becomes larger as the flow rate is decelerated.

Ameri et al. [11] determined that the leakage flow rate is reduced by the cavity tip for the axial turbine about 10-14% confining the vorticity within the cavity. K. Du et al. [12] has shown that the

cavity tip reduces the leakage flow loss by up to 6.1% by applying the intermittent multi cavity structure.

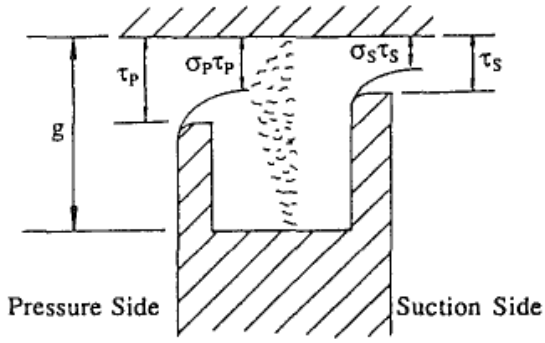

Figure 2.4 Leakage flow simplification model through the cavity tip [13]

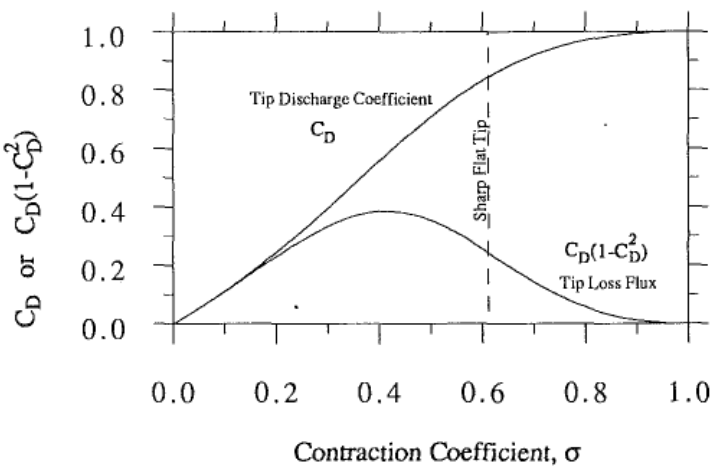

Figure 2.5 Tip discharge coefficient and tip loss flux as a function of contraction coefficient [13]

Also, Figure 2.4 indicates that Heyes [13] applied a fillet to the

pressure side tip edge to eliminate the pressure side tip leakage vortex that occurs when the tip leakage flow passes through the angled pressure side tip edge. The loss inside the tip was reduced, but contrary to the expected effect, the flow constriction was less due to the effect of the tip radius and the leakage flow rate increased as shown in Figure 2.5. As a result, the flow coefficient is minimal at sharp corners and the leakage flow is also minimized.

Winglet Tip

A winglet tip was introduced to reduce the leakage flow by reducing the pressure difference between the pressure side and the suction side. In the case of the pressure side winglet, since the pressure gradient in the pitchwise direction is not large, the effect of reducing the discharge coefficient is dominant, whereas the suction side winglet has a relatively large pressure gradient, which is more effective in reducing the pressure difference between the pressure side and the suction side in the tip gap. However, as the suction side is expanded by the winglet structure, it may be easily affected by the tip leakage vortex, and the leakage flow rather increases depending on the installation location [14].

2.3.3 Radial Turbine Tip Leakage Flow Reduction

For a radial turbine, Shao et al. [15] applied cavity on its rotor shroud to reduce the leakage mass flow rate by increasing the rotating speed or decreasing the seal clearance. Tamaki et al. [16] showed that smaller opening area of the radial turbine VGN increases its leakage mass flow rate as the setting angle of the nozzle blade is increased, and analyzed the effect of the leakage flow on the rotor.

Many CFD studies have been conducted on the radial turbine VGN including analysis of the aerodynamic performance by changing the blade profile while maintaining the same chord and the number of blades Chen and Huang, [17], or comparing the blade thickness and solidity while maintaining the throat area and the chord by Yang [18].

Chapter 3. Modelling Analysis and Selection of Tip Design

In this research, to confirm the same flow mechanism like the axial turbine, the tip designs which showed effective tip leakage flow reduction in the previous research are applied to the radial expander VGN. Before applying these tip designs, the discharge coefficients of each design were derived and compared.

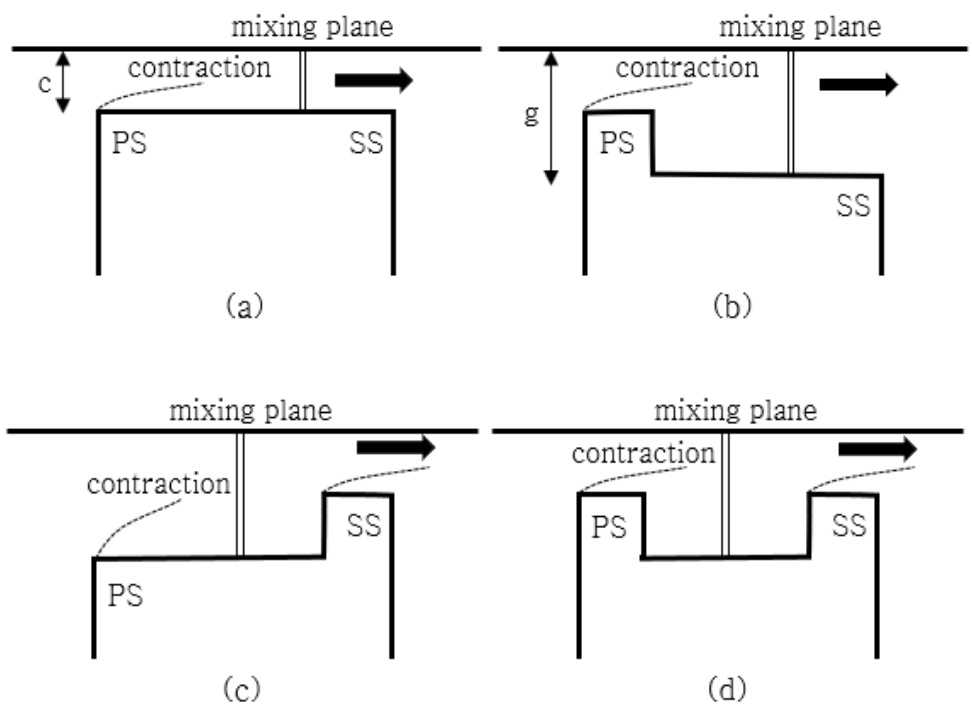

Figure 3.1 Tip design (a) Flat tip (b) Pressure side squealer tip (c) Suction side squealer tip (d) Cavity tip

The discharge coefficients of each tip design shown in Figure 3.1 are derived as follows, ignoring shear at the tip surface and applying the law of conservation of mass and momentum to the vena contracta of the pressure side and the tip gap outlet of the suction side.

- Flat tip, $C_D = \frac{\sigma}{\sqrt{1+2\sigma^2-2\sigma}}$
- Pressure side squealer tip, $C_D = \frac{\sigma}{\sqrt{1+2\frac{c^2}{g^2}\sigma^2-2\frac{c}{g}\sigma}}$
- Suction side squealer tip, $C_D = \frac{\sigma}{\sqrt{1+\sigma^2-2\sigma+\frac{g^2}{c^2}}}\frac{g}{c}$
- Cavity tip, $C_D = \frac{\sigma}{\sqrt{2+\frac{c^2}{g^2}\sigma^2-2\frac{c}{g}\sigma}}$

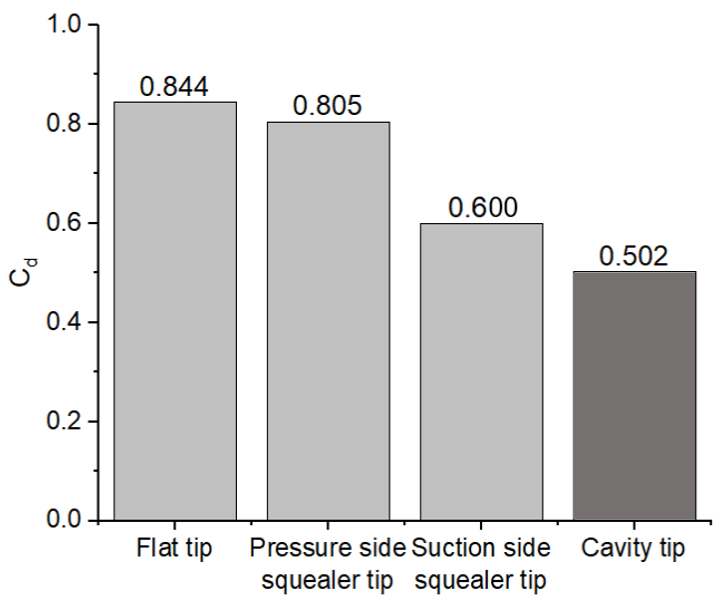

Figure 3.2 Discharge coefficient of each tip design

Figure 3.2 shows each discharge coefficient of each tip design. For the contraction coefficient(σ), a theoretical value of 0.611 obtained from potential flow was used, and the c/g value was substituted for 2 assuming that the squealer base was cut by the tip gap.

The discharge coefficient of the flat tip is the largest of 0.844 so that the leakage flow rate is also the largest, to which the tip design is not applied. As in the previous research, the suction side squealer tip is more effective in reducing the leakage flow than the pressure side squealer, it can be seen that the discharge coefficient of the suction side squealer tip is 0.600 rather than that of 0.805 of the pressure side squealer tip. In the case of the cavity tip, the discharge coefficient is 0.502, which can be predicted to be more effective in reducing the leakage flow than when the squealer tip is applied. Therefore, in this research, the cavity tip was applied to the radial expander VGN to verify the cavity tip effect and the tip leakage flow reduction.

Chapter 4. Computational Setup

4.1 Numerical Method

Commercial program ANSYS CFX 2019 R1 was used for solving three-dimensional steady state Reynolds-averaged Navier-Stokes equations. The k-ω SST model was adopted because it is suitable for both boundary layer and free stream analysis.

Table 4.1 General numerical setting

Grid / Solver	ANSYS ICEM (stator), Turbo grid (rotor) / ANSYS CFX
Number of elements	2.4 millions (rotor)
Turbulence model	SST
Simulation type	3D, steady state
Fluid material	N2 (Dry Redlich Kwong)
Inlet boundary condition	total pressure, total temperature
Outlet boundary condition	static pressure

4.2 Computational Domain

In this research, as shown in Figure 4.1, the radial expander consists of 15 stator (VGN) blades and 14 rotor blades but the computational domain includes one blade for each the rotor and the stator, giving periodic boundary conditions to one blade passage at

the circumferential interface. The stator blade has 0.1 mm of the tip clearances at both hub and shroud side and its span is 4.5 mm, and the rotor blade has 0.4 mm of the tip clearance only at the shroud side.

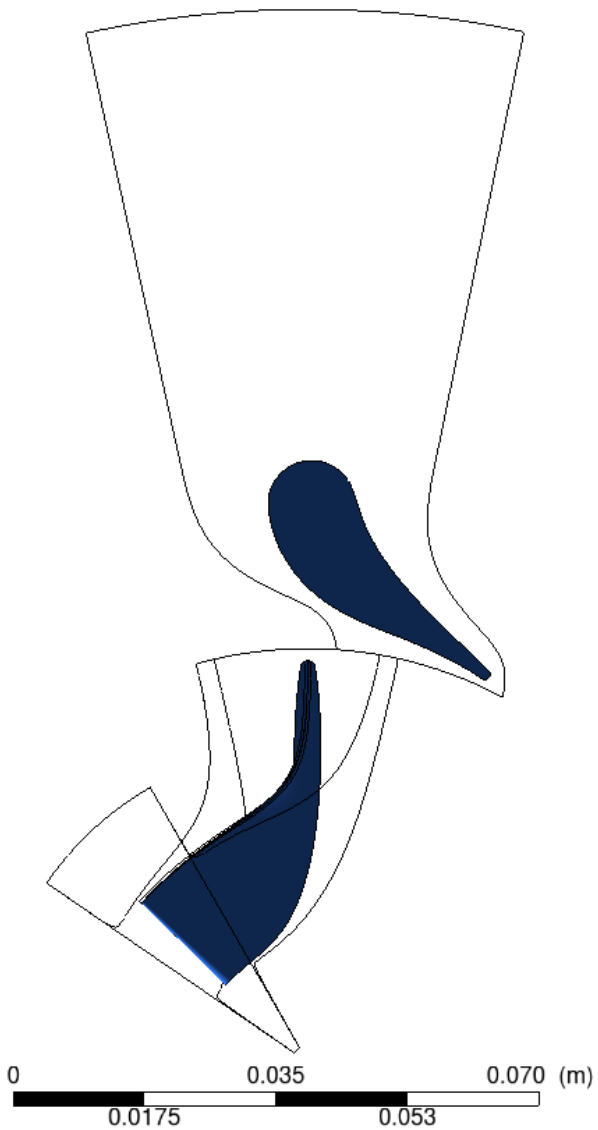

Figure 4.1 Partial stator-rotor domain with periodic boundary condition

4.3 Boundary Conditions

For boundary conditions, a total pressure of 4040 kPa and a total temperature of 162.15 K were set to the inlet, and a static pressure of 970 kPa to the outlet. The rotating speed of rotor was 36947 rpm. Fluid material was N2 and Dry Redlich Kwong material was used. The interface between the rotor and the stator is set as a mixing plane.

4.4 Convergence Method

In order to solve the problem that the simulation is easily divergent due to the relatively large expansion ratio and rotor speed, the idea of a step-by-step convergence method was applied. The step-by-step convergence method is by first setting a higher static outlet pressure and a lower rotor speed than the target design point to induce convergence, and then setting this converged result file as an initial condition to the next simulation which has lower outlet static pressure and higher rotor speed. This method can prevent divergence of simulation due to the occurrence of negative feedback as the initial condition randomly added by CFX being inappropriate for the extreme boundary condition. In this research, the simulation was divided into a total of 6 steps with the boundary conditions shown in Table 4.2 below, and the result convergence

was induced step-by-step.

Table 4.2 Boundary condition using step-by-step convergence method

Step	Outlet static pressure (kPa)	Rotorating speed (rpm)
1	2800	15000
2	2300	20000
3	1900	25000
4	1450	30000
5	1200	33000
6 (Final)	970	36947

4.5 Mesh

4.5.1 CFX Grid Generation Method

Proper grid selection is essential because the size and number of grids affect the resulting accuracy/computation speed. In general, as the number of nodes increases, the result accuracy improves, and since degrees of freedom are calculated for each node, an increase in the number of nodes leads to a decrease in the calculation speed.

ANSYS CFX used in this project is a node-based solver that builds a control volume around the nodes of the grid and stores the calculated result values in the nodes. CFX has an advantage in fluid

analysis reliability over other CFD software by creating a denser grid by adding a sub-lattice between nodes by itself. As shown in Figure 4.2 below, the number of integration points is doubled from 4 to 8 in the same control volume, improving the calculation precision.

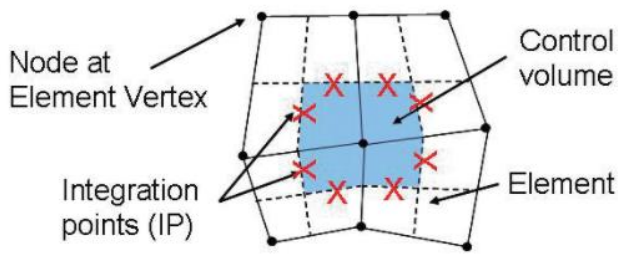

Figure 4.2 ANSYS CFX Sub-Grid Creation Schematic

4.5.2 Grid Types

However, the number of nodes is not always an absolute criterion, and the result accuracy/calculation speed varies depending on the type of element. In this project, a rectangular grid (Hexa mesh) and a triangular grid (Tetra mesh) were selected and used according to the degree of complexity of the shape. In CFX used for analysis, when the control volume of a rectangular grid is built, 6*4=24 integration points are generated on 6 sides of the rectangular grid control volume, but in the case of a triangular grid, approximately depending on the number of tetra and prism elements created. An integral point of 2-3 times is created. Accordingly, the amount of numerical calculation also increases with the triangular grid.

Due to the characteristics of fluids with greater continuity compared to solids, numerical diffusion can be caused in Eulerian numerical analysis using a discrete grid. Because the irregular grid is not aligned with the flow direction of the fluid, it is calculated in a different direction from the actual flow between the grids, leading to non-physical results. In the triangular lattice, which is an irregular lattice, the inaccuracy due to this diffusion is relatively high.

However, if you use enough nodes, you can get the same result with a triangular lattice as a rectangular lattice. In particular, when analyzing complex shapes, the time required to create a rectangular grid that cannot be automatically generated is enormous. In this case, it may be more economical to use a triangular grid that is relatively easy to create and increase the CPU time for calculation.

4.5.3 Mesh Characteristics and Generation

All stator mesh that design factors are applied uses the commercial program ANSYS ICEM, and the rotor mesh is unified by using ANSYS Turbo Grid. The hexahedral mesh was adopted because numerical diffusion occurs in Eulerian numerical analysis so that the unstructured mesh such as tetrahedral mesh can lead to non-physical results as which is not aligned with the actual flow direction. To obtain detailed flow analysis near the wall, O-grid

mesh is adopted around the stator blade walls and inflation layer is adopted for all surfaces. Also, the 'automatic near wall treatment' function which is supported by ANSYS CFX is adopted to ensure achieving proper wall treatment according to the y+ value at each wall.

4.5.4 Mesh Independence Test

Mesh independence test is carried out for the single cavity model by changing the number of elements and comparing their efficiency. The number of elements used for verification is 9.9 million, 13.8 million, and 16.2 million. As shown in Figure 4.3, errors are less than 0.5% so that the convergence was sufficiently independent of the increase or decrease of the number of elements.

However, in the case of 9.9 million mesh, it shows relatively poor residual convergence, which can affect the accuracy of the analysis results, so the simulations are performed based on 13.8 million mesh.

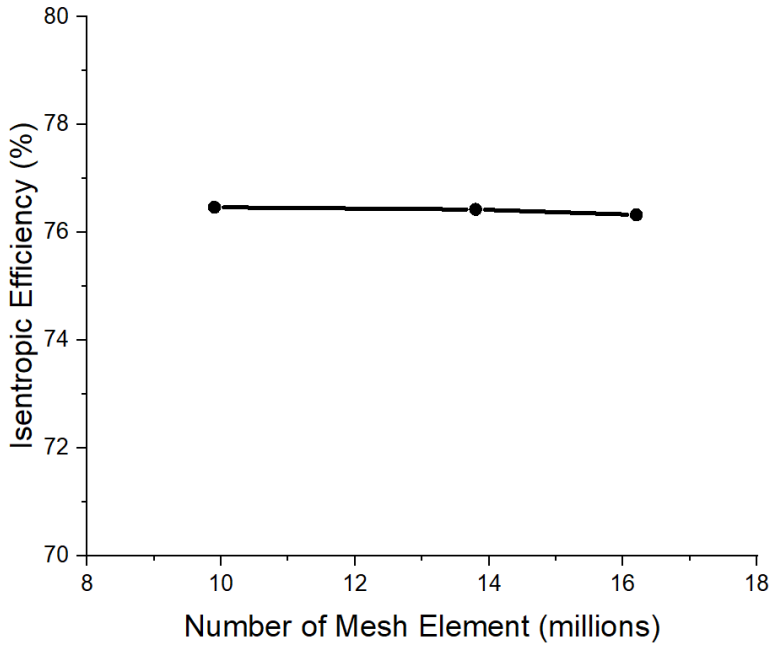

Figure 4.3 Mesh independence test

Chapter 5. Tip Design Applications and Discussion

5.1 Flat tip

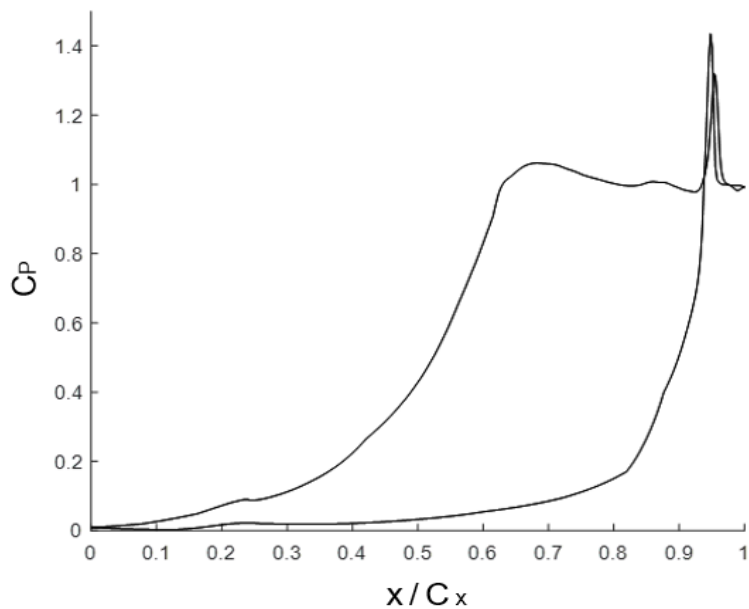

Figure 5.1 Flat tip case Blade loading at 50% span

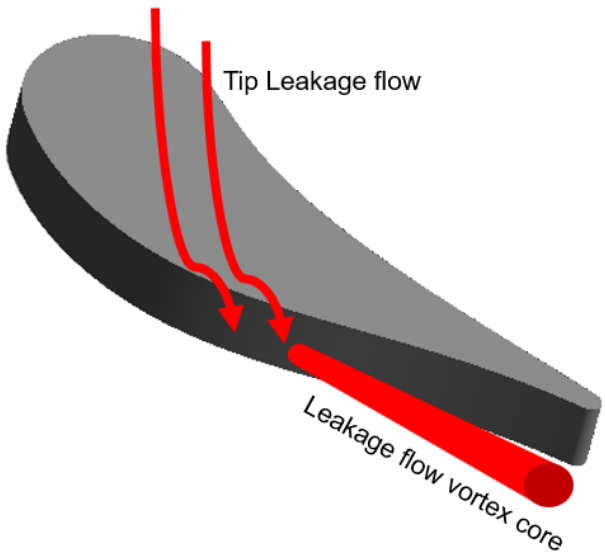

Figure 5.2 Flat tip case Tip Leakage Flow Schematic

Figure 5.1 above is the blade loading calculated at 50% span of the blade in the flat tip case. The x-axis is the normalized length from the leading edge of the blade to the trailing edge in the chord direction, and the y-axis is the pressure coefficient which is nondimensionalized by the stator inlet total pressure (P_{01}) and the outlet static pressure (P_2). It can be seen that the static pressure measured on the pressure side is maintained up to the 80% chord and then falls, while that measured on the suction side falls sharply from 20~30% chord, so that the blade loading is concentrated on the trailing edge side. It can be predicted that the leakage flow will more likely to flow from the pressure side to the suction side changing its direction drastically at the trailing edge (20-100%)

part where the blade loading is concentrated.

5.1.1 Tip Leakage Flow Rate Calculation

The streamline in the Figure 5.3 (a) shows that the inflow angle into the tip gap varies depending on the region due to the influence of the blade loading and the blade angle. At 20~100% chord, the leakage flow flows from the pressure side to the suction side and the inflow angle is close to perpendicular to the chordwise direction, whereas at the part close to the leading edge (0~20% chord), the leakage flow is almost parallel to the chordwise direction. Therefore, in order to consider the effect of the inflow angle on the leakage flow, the leakage flow rate is calculated by dividing the parts as shown in Figure 5.3 (b).

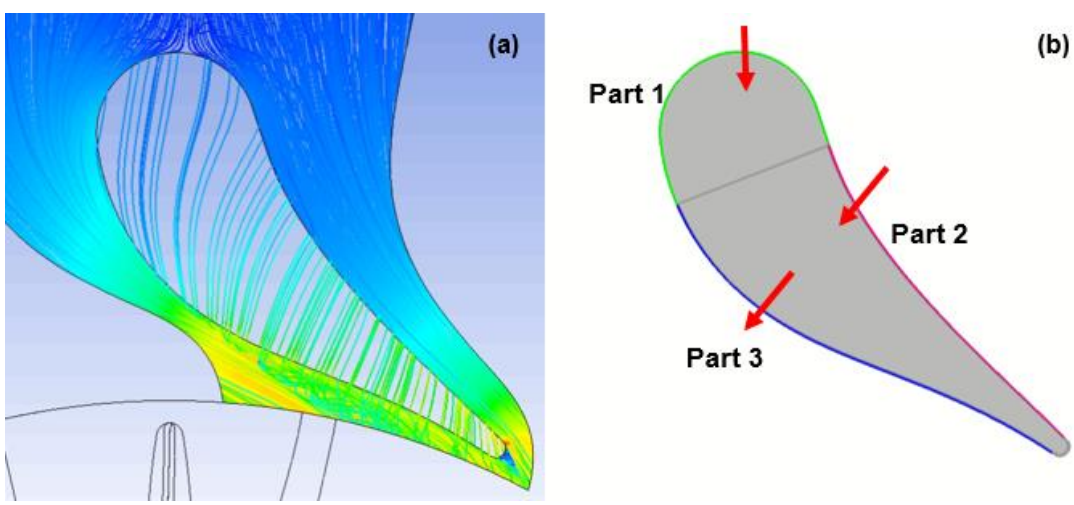

Figure 5.3 Flat tip (a) Streamline (b) Part division for leakage flow rate calculation

5.2 Cavity Tip Application

In this research, the single cavity tip and the multi-cavity tip were applied to confirm the effect of cavity tip (Figure 6).

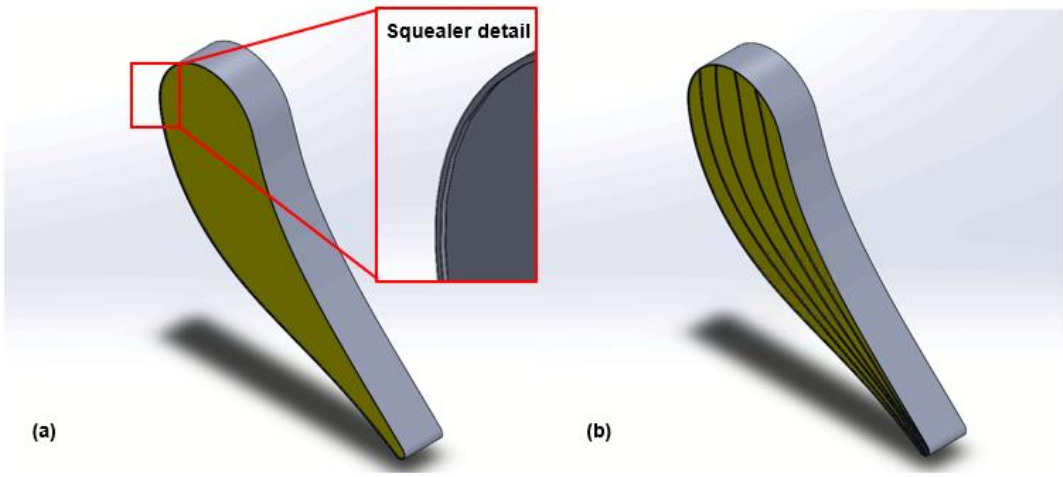

Figure 5.4 Geometry (a) Modified single cavity tip

(b) Multi cavity tip

5.2.1 Single Cavity Tip

Efficiency changes were compared for single cavity shapes by varying the depth of the cavity tip and the thickness of the cavity squealer. The squealer thickness when changing the cavity depth was fixed at 2 mm, and the cavity depth when changing the squealer thickness was fixed at 0.1 mm.

All of the single cavity analysis used Hexa grids, and the number of grids was maintained at 13 to 14 million.

Table 5.1 Efficiency variation with cavity depth and squealer thickness

Case	Efficiency (%)	Efficiency change (%p)
Flat tip	76.55	0
Depth 0.05 mm	76.52	-0.03
Depth 0.1 mm	76.43	-0.12
Depth 0.2 mm	76.35	-0.20
Depth 0.5 mm	75.78	-0.77
Squealer 0.1 mm	76.61	+0.06
Squealer 0.5 mm	76.10	-0.45
Squealer 2 mm	76.43	-0.12

As a result of performing the analysis by changing the cavity tip depth to 0.05 mm, 0.1 mm, 0.2 mm, and 0.5 mm, the efficiency tends to decrease as the cavity tip deepens. The depth 0.05mm case, which is the shallowest cavity tip, also had an efficiency of 76.52%, which was lower than that of the baseline case of 76.55%.

As shown in the previous study, the leakage flow passes through the top of the squealer on the pressure side and the suction side, and two flow contractions occur inside the cavity, resulting in mixing loss. An increase in entropy can be observed. However, it was confirmed that there is a point where the shear stress becomes 0 at the top of the squealer tip, and it was inferred that flow

reattachment occurred at this point. This point is located at a distance of about 0.1 to 0.2 mm from the inlet of the gap into which the leak flow entered.

To prevent flow reattachment at the top of the squealer tip, analysis was performed by reducing the cavity squealer thickness to 2 mm, 0.5 mm, and 0.1 mm, and it was confirmed that there was no flow reattachment only at 0.1 mm. As the thickness of the squealer was decreased, the efficiency decreased as shown in Table 5.1, and only the squealer 0.1 mm case in which flow reattachment did not occur. The efficiency slightly increased to 76.61%, but the efficiency was actually increased with a slight difference (<<0.1%). It cannot be confirmed that the improvement has been made.

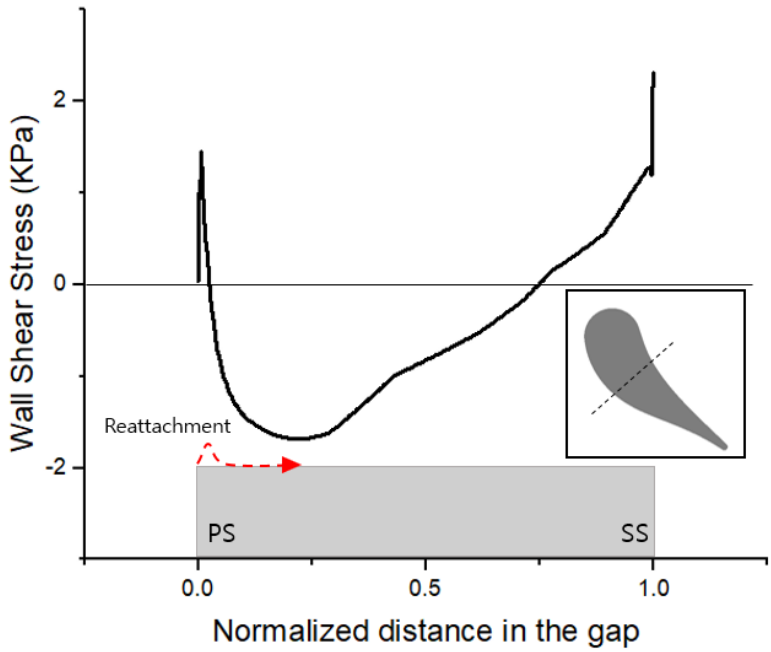

Figure 5.5 Flat tip wall shear stress of tip surface

According to the previous research by Schabowski et al. [9], the selection of a squealer thickness which is thin enough to prevent reattachment in the tip gap. Figure 5.5 shows the wall shear stress at the top surface of the flat tip blade, and the x−axis is the length in mm from the pressure side to the suction side at 50% chord of the blade. It can be inferred that flow reattachment occurs around 0.2 mm, the point at which the wall shear stress first becomes zero from the pressure side. This is consistent with the research of (Sjolander and Cao [4], that the flow entering the tip gap reattached at the 2.4τ point. Also, the leakage flow reattachment can be seen from the Mach number contour in Figure 5.6 (a). Therefore,

simulations were performed by modeling the cavity tip with a squealer thickness of 0.1 mm, which is 1x of the tip gap width. In Figure 5.6 (b), the Mach number contour shows the leakage flow reattachment does not appear at the top surface of the squealer of the multi cavity tip case. By preventing reattachment at the squealer, the pressure drop in the vena contracta can be decreased and ultimately the tip clearance loss can be reduced.

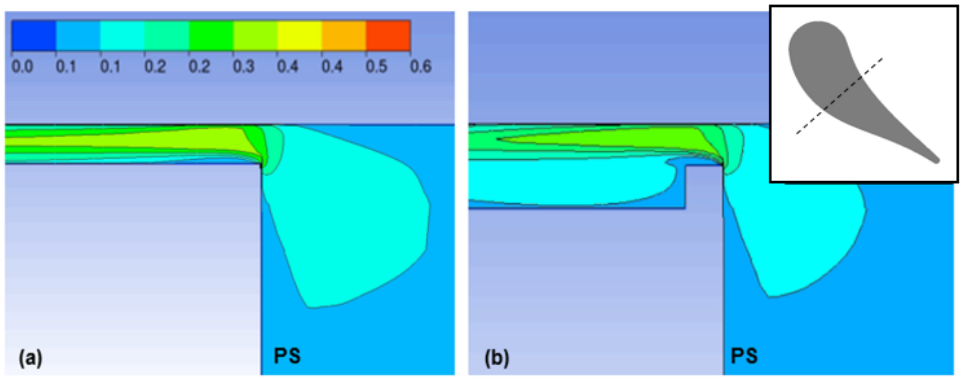

Figure 5.6 Mach number contour in tip gap (a) Flat tip (b) Single cavity tip

Table 5.2 Leakage flow rate of single cavity tip

Section	Flat tip (kg/s)	Single cavity tip (kg/s)
Part 1	-0.0028	-0.0069
Part 2	-0.0168	-0.0177
Part 3	0.0196	0.0246

Therefore, 0.1 mm squealer tip case was chosen as single cavity tip case and the cavity tip flow characteristics occurred such as flow contraction at the squealer and mixing process inside the cavity as in the previous research. However, there was no significant change of the total leakage flow rate compared to the flat tip case (0.0198kg/s to 0.0205 kg/s) (Table 5.2).

The difference from previous research, where the efficiency was improved by applying a cavity tip, is that the VGN blade is about two times thicker than the general turbine rotor blade, and the VGN is a non-rotating stator unlike turbine rotor. Due to the relatively thick blade, the effect of friction loss is dominant inside the cavity with a relatively large cavity area compared to previous research. Thus, more the leakage flow is induced to offset the pressure increase inside the cavity so that there is little change in the leakage flow rate compared to the flat tip case. Also, because it does not rotate, the scraping vortex is not formed inside the cavity so that a labyrinth seal effect is much lessen as shown in Figure 5.7 (b). As these differences from previous research exist, the effect of the cavity tip was not applied.

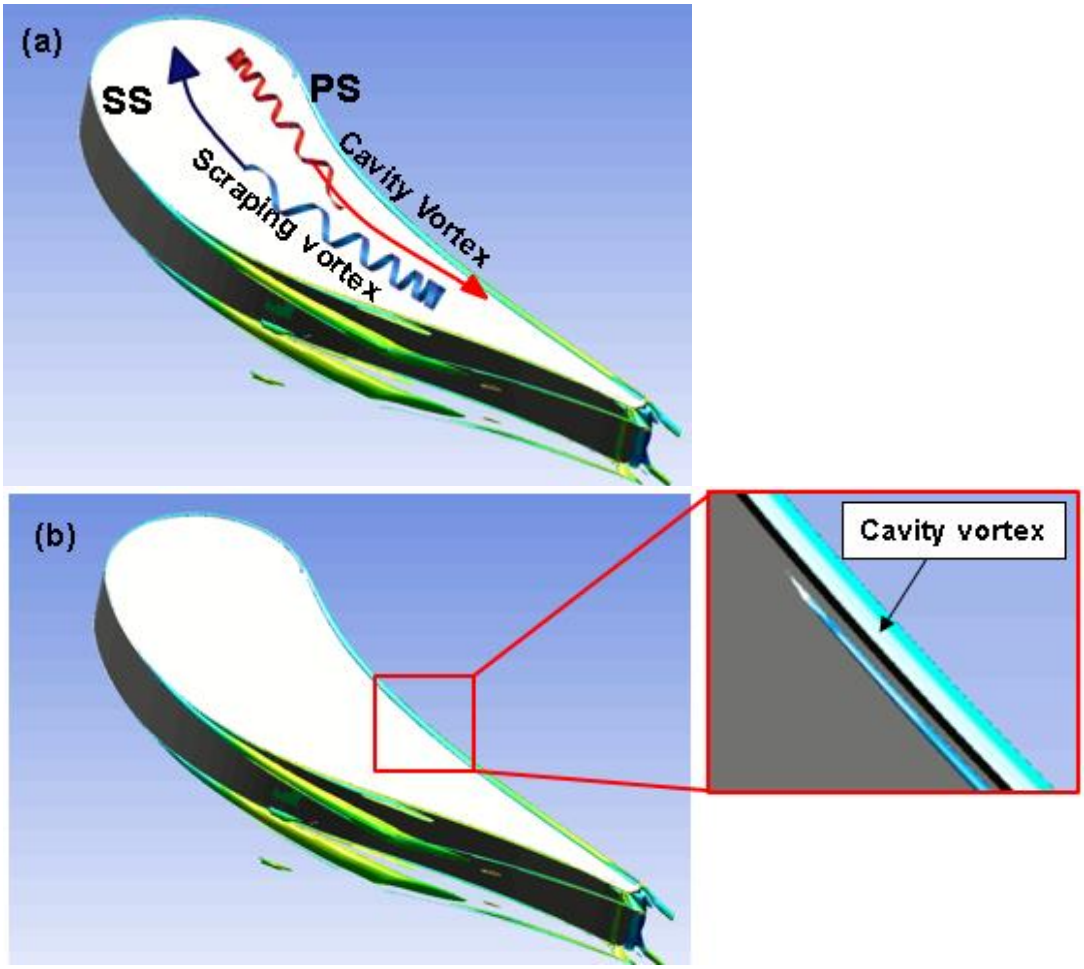

Figure 5.7 vortex of single cavity tip on (a) axial expander rotor blade (b) radial expander VGN

5.2.2 Multi-Cavity tip

The multi cavity tip idea was applied to induce the cavity effect on the thicker blade. In contrast to the existing multi cavity tip which splits the cavity in the chordwise direction proposed by K. Du et al. [12], the multi cavity tip in this research is splitting the cavity intermittently in the direction of the leakage flow passage. The idea

of the multi cavity tip is constructing blade shape similar to connecting several thin blades together so that compensating for the lack of cavity effect due to the relatively thick blade. By applying multiple pressure drops from each small cavity tip, the cavity effect is expected to be increased such as the vena contracta and mixing process rather than the effect of frictional loss.

By applying the multi cavity tip, the efficiency was increased by 1.25 %p compared to the flat tip case.

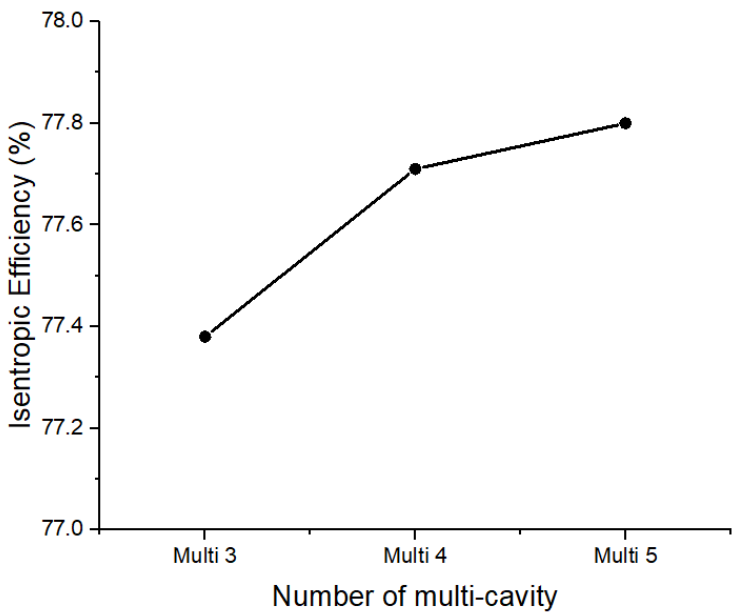

Figure 5.8 The efficiency trend of the number of multi-cavities

As the number of multi-cavities was changed to 3, 4 and 5, respectively, the efficiency tends to increase as the number increases. However, comparing multi 4 and multi 5 cases, the

difference is less than 0.1%p. Thus, when the number of multi-cavities is 5 or more, it can be predicted that converges to the optimum value numerically.

5.2.3 The Leakage Flow of Multi-Cavity Tip

Table 5.3 Leakage flow rate of Multi-cavity tip

Section	Flat tip(kg/s)	Multi-cavity(kg/s)
Part 1	-0.0028	-0.0065
Part 2	-0.0168	-0.0144
Part 3	0.0196	0.0209

However, there was little change the total leakage flow rate from part 3 as shown in Table 5.3. The reason is that the leakage flow from the leading edge side (0~20% chord) is increased in part 1 and the leakage flow is decreased due to the cavity effect in part 2 (Table 5.3). Figure 5.9 is a graph showing the leakage flow entering the pressure side along the chordwise direction from the leading edge to the trailing edge. Compared to the flat tip case, the multi cavity tip showed a tendency to increase the flow rate at the leading edge side and decrease at the trailing edge side based on 50% chord. By applying cavity to the leading edge side (0~20%), the rapid acceleration of the flow occurred due to the cavity when the

leakage flow passed through the squealer tip, so that the leakage flow rate is increased. From this, it can be estimated that when the flow angle of the leakage flow is parallel to the chordwise direction, the adverse effect of the cavity occurs and increases the leakage flow rate in that section. Therefore, the cavity effect can be confirmed by limiting it to part 2.

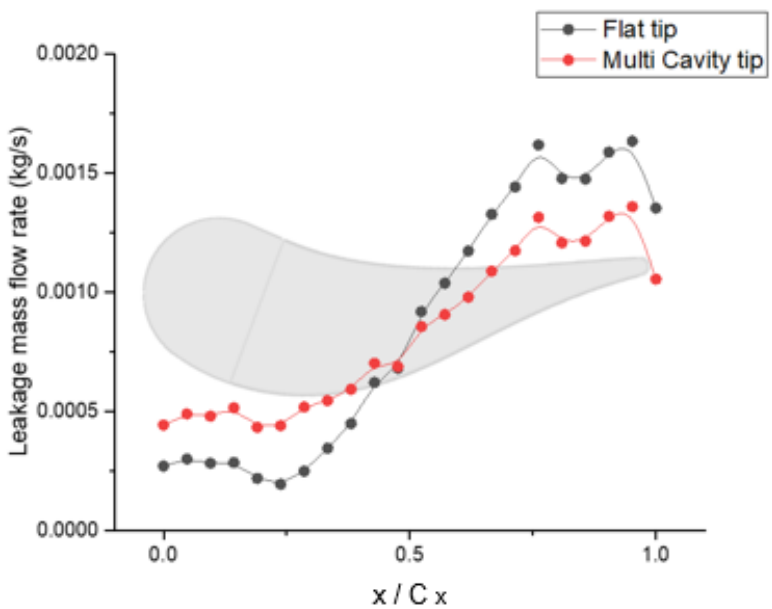

Figure 5.9 Leakage mass flow rate of flat tip and multi cavity tip

In addition, as the core region of the leakage flow vortex is moved shown in Figure 5.10, the bulk flow angle at the VGN outlet is decreased by about 1 degree with decreased tangential velocity and increased axial velocity. Therefore, it can be estimated that the loss

reduction was caused by a combination of decreased leakage flow rate in part 2 and the change of the nozzle exit angle.

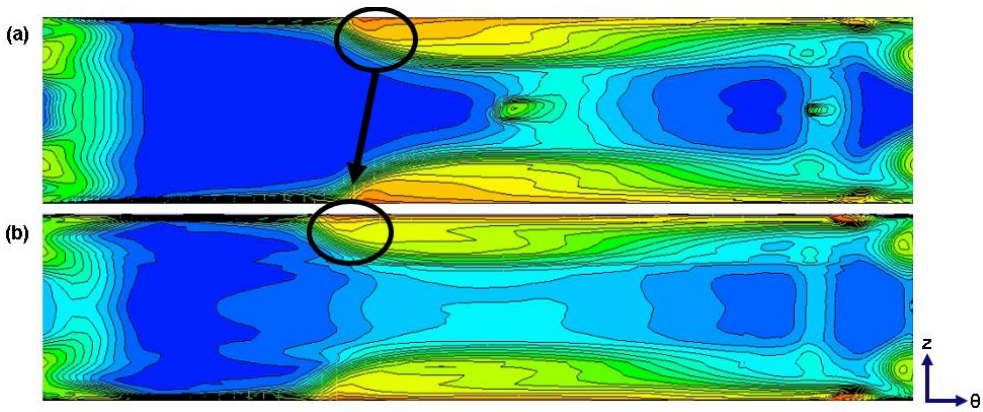

Figure 5.10 Total pressure loss coefficient at VGN outlet

Total pressure loss coefficient = $(P_{01} - P_{02})/(P_{02} - P_2)$

5.3 Leading Edge Blocking Tip

Table 5.4 Leakage flow rate of single cavity tip with leading edge blocking

Section	Flat tip(kg/s)	Single cavity(kg/s)	LE block Single cavity(kg/s)
Part 1	-0.0028	-0.0069	-0.0044
Part 2	-0.0168	-0.0177	-0.0187
Part 3	0.0196	0.0246	0.0231

Table 5.5 Leakage flow rat of multi−cavity tip

with leading edge blocking

Section	Flat tip(kg/s)	Multi-cavity(kg/s)	LE block Multi-cavity(kg/s)
Part 1	-0.0028	-0.0065	-0.0032
Part 2	-0.0168	-0.0144	-0.0109
Part 3	0.0196	0.0209	0.0141

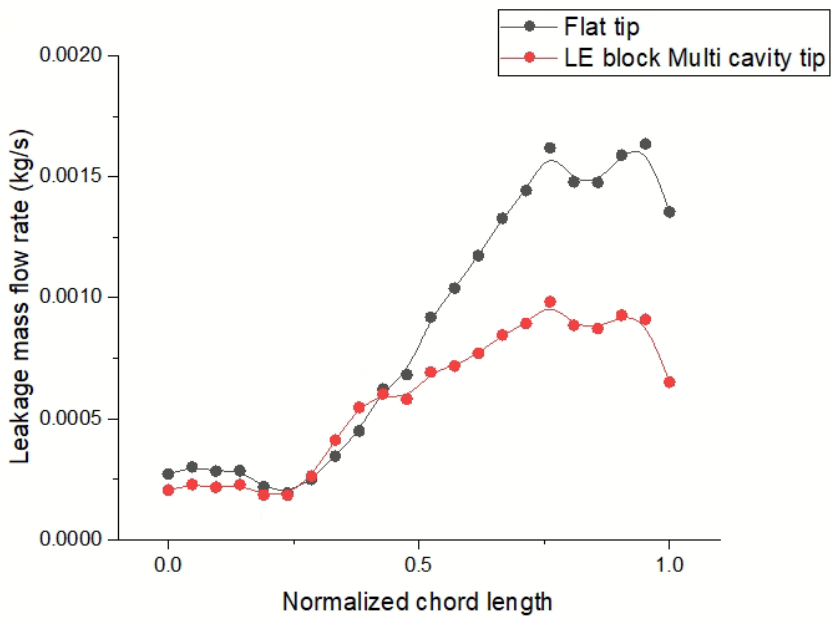

Figure 5.11 Leakage mass flow rate of flat tip and multi−cavity tip

with leading edge blocking

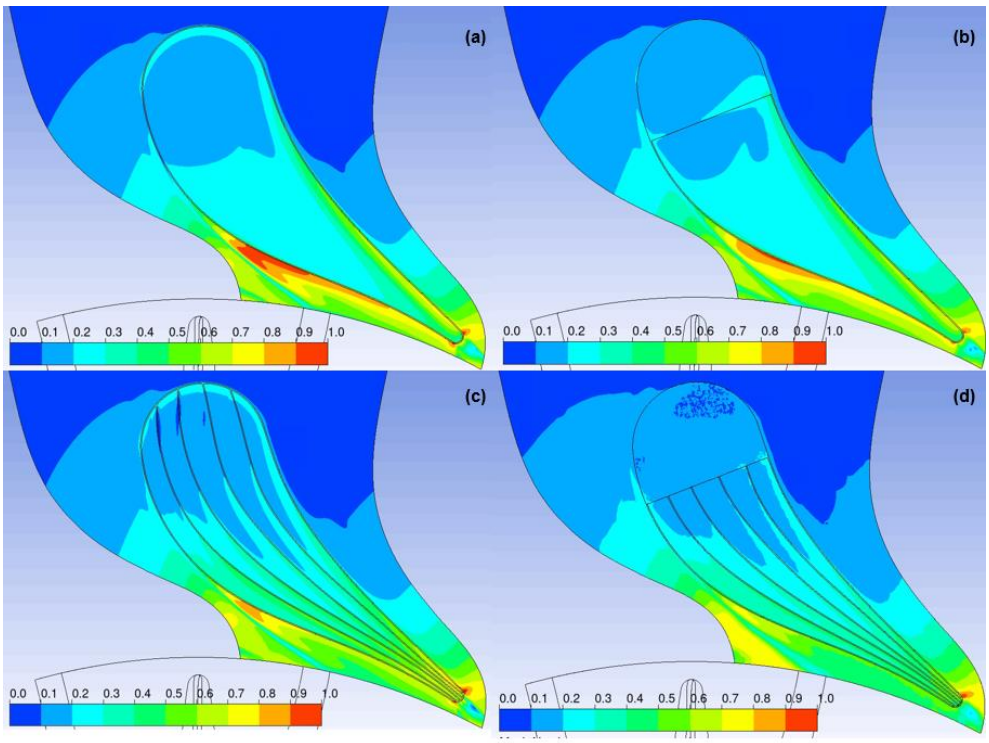

Figure 5.12 Mach number contour (a) Flat tip (b) Flat tip with leading edge blocking (c) Multi-cavity tip (d) Multi-cavity tip with leading edge blocking

When the multi-cavity tip is applied, it is necessary to block the leakage flow in part 1 to confirm the loss reduction due to the leakage flow reduction in part 2 alone. Therefore, the idea of minimizing the effect of the increased leakage flow rate in part 1 was applied by blocking the dented cavity region of part 1. Figure 5.11 shows that the leading edge of a multi-cavity is blocked. Compared to the flat tip case, the efficiency of the leading edge blocking single cavity tip case increased by 0.3%p and that of multi-cavity tip case increased by 1.25%p. Table 5.4 and 5.5 show

that the leakage flow of part 1 is reduced by blocking the leading edge in both cases compared to the original cases in which the leading edge is not blocked. In the case of the single cavity tip, since the leakage flow rate of both part 1 and part 2 increased compared to the flat tip case, it can be seen that the efficiency shows little change only by changing the nozzle exit angle without cavity effect. In the case of the multi-cavity tip, the total leakage flow rate of part 3 decreased compared to the flat tip case. It can be confirmed that the multi-cavity tip reduces the leakage flow rate in part 2 and thus the leakage flow loss is reduced.

As shown in the figure 10 (a), in the absence of the leading edge blocking, a rapid acceleration of the flow occurs due to the cavity passing through the squealer tip of the leading edge, and the leakage flow rate of part 1 increases. By blocking part 1, the Mach number of the vortex formed in the suction side decreases by preventing the acceleration of this leakage flow and reducing the leakage flow. From this, it can be seen that as the cavity tip is applied, when the flow angle of the leakage flow is parallel to the code direction, the reverse effect of increasing the leakage flow rate acts, and it can be prevented by blocking the cavity of the corresponding part.

In addition, when comparing the stage loss of VGN, it decreased by

2.73% for the multi-cavity tip and 4.19% for the multi-cavity with leading edge case. This shows a result corresponding to the generation of entropy (Table 5.6).

Table 5.6 VGN entropy generation and stage loss

VGN (stator)	Flat tip	Multi-cavity	LE block Multi-cavity
Entropy generagtion	-	-3.31 %	-4.91 %
Stage loss	-	-2.73 %	-4.19 %

Stage loss coefficient = $(P_{01} - P_{02})/\frac{1}{2}\rho V^2$

Chapter 6. Additional Tip Designs

6.1 Winglet Tip

By applying the winglet on VGN, same effect in the axial flow turbine in the previous study was confirmed. The main goal was to reduce the leakage flow by reducing the pressure difference between the pressure side and the suction side, and considering the narrow gap between the blades, a winglet was added only to the suction side with a relatively large pressure gradient.

The width of the winglet was maintained at 1.45 mm in the middle of the blade and modeled to gradually narrow at 20% chords from the leading and trailing edges, respectively, to minimize the resistance of the main flow flow. The thickness of the winglet was modeled to gradually decrease from 0.5 mm to 0.1 mm to prevent shape deformation during processing and heat treatment.

The winglet case uses a tetra grid in order to shorten the working time with many narrow curves. The number of Tetra grids is 7.9 million. The grid difference was considered by comparing the efficiency with the tetra grid flat tip case.

The winglet shows an effect of increasing efficiency by about 1%p.

In multi-cavity, the leakage flow rate at the leading edge increased and the leakage flow rate decreased significantly at the trailing edge based on the 50% code, whereas the overall flow rate of the winglet showed a tendency to decrease. Also, there is almost no change in the leakage flow rate near the 60% cord. It is assumed that the suction surface pressure decreases due to the influence of the vortex generated at the trailing edge of the adjacent blade located near the 60% cord suction surface.

6.2 Cavity-Winglet Tip

Analysis was performed by merging the multi-cavity and winglet shape, which had the effect of improving efficiency. In order to clearly understand the interference that may occur when two cases are merged, the shapes of the Multi 5 case and the Winglet case were applied together without modification and modeled.

The cavity-winglet tip case includes a winglet shape with a lot of narrowing curves, so a tetra grid was used to shorten the working time. The number of tetra grids is 9 million. The grid difference was considered by comparing the efficiency with the tetra grid flat tip case.

In the cavity-winglet tip case, the efficiency was increased by about 2.2%p compared to the baseline case. Considering that Multi

5 case has an efficiency increase of 1.2%p and winglet case 1%p compared to the baseline case, it can be inferred that the multi-cavity and the winglet operate independently without interfering with each other.

The leakage flow was increased at the leading edge based on the 50% code, but less leakage flow was confirmed than the multi-cavity due to the influence of the winglet. At the trailing edge, the multi-cavity and the winglet acted in a complex way, and the leakage flow was greatly reduced.

Considering the convergence of the efficiencies in the 5 multi-cavities, it can be seen that adding a multi-cavity to the upper part of the extended tip will show a similar increase in efficiency. In addition, if the cavity of the leading edge part is blocked, it is also expected to act independently of the winglet and increase the efficiency.

6.3 Tip Roughness

As in the flat tip, the pressure of the blade shape of this project decreases due to the continuous frictional loss in the tip gap. From this, a method for further increasing friction loss was conceived. When the friction loss of the blade tip increases, the pressure loss coefficient graph rises with a steep slope, and the pressure

decreases steeply at the top of the blade tip. To compensate for this steep decrease in pressure, it can be expected that there will be less pressure drop in the axial vein as the leakage flow enters the pressure side.

In order to increase the friction loss of the blade tip, the surface roughness of the blade tip portion was increased from the existing roughness of 19 microns to 57 microns and 95 microns, and the other surfaces were maintained at 19 microns. Roughness changed the surface roughness setting in the process of creating the def file in CFX. The grid was kept the same at the level of 13.8 million Hexa grids.

The roughness function in CFX uses a method of calculating the additional shear induced by the roughness by transforming it in the log law region of the wall function. The transformed wall function is as below.

$$U^+ = \frac{1}{\kappa}\log(Ey^+) - \Delta B$$

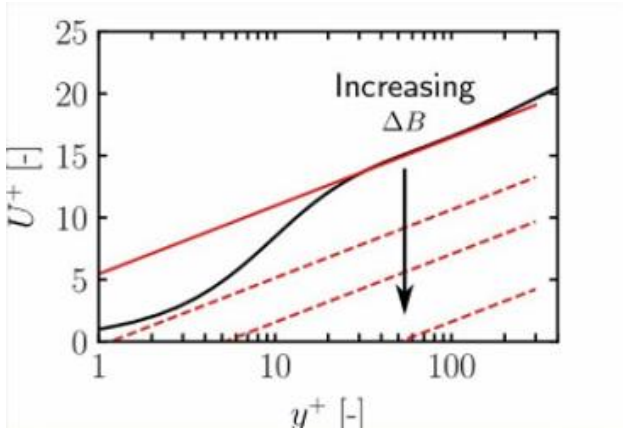

Figure 6.1 Wall function for increasing surface roughness

The added function ΔB depends on the shape and size of the roughness.

This function is generally used when the roughness height is smaller than the first node size on the wall. However, since the model of this project has a relatively narrow tip gap compared to the roughness height, there is a possibility that the result value of speed or pressure may be inaccurate if calculated by simply transforming the wall function. In order to obtain accurate results, fine modeling of the surface is required.

As a result of changing the surface roughness of the blade tip, the Rough 57 case increased by 0.16%p and the Rough 95 case by 0.22%p compared to the flat tip case.

However, compared with the tip gap, which is a narrow gap of 0.1 mm, the roughness height of the Rough 57 case is more than half of the gap size, and the roughness height of the Rough 95 case is

almost the same as the gap size. As mentioned earlier, under these conditions, the reliability of CFX analysis may drop, and in reality, casing and wear/jamming may occur during operation, so it is not considered suitable.

Chapter 7. Conclusions

In the present research, to reduce the leakage flow rate in the VGN tip clearance, the cavity tip was selected as a design factor based on the paper review of previous research related to the turbine rotor blade to predict the leakage flow rate reduction. CFD analysis was performed by applying the cavity tip to the VGN of the radial expander to check the tip leakage flow rate at the pressure, the suction, and the leading edge side each.

In the radial expander VGN blade, unlike the axial turbine rotor blade, the difference in flow structure was appeared such that frictional loss is dominant and the trailing vortex is not formed. Thus, application of the multi-cavity tip idea to a VGN blade could induce the cavity effect at the trailing edge side. The efficiency of the multi-cavity tip is increased by 1.25%p compared to the flat tip. Also, as over 27%p of the total tip leakage flow rate was induced by the inflow at the leading edge side, blocking the leading edge side was applied both single and multi-cavity tip to confirm the cavity tip effect only at the pressure side. The efficiency of the leading edge blocking multi-cavity tip is increased by 1.84%p compared to

the flat tip.

Through this research, it can be seen that, when the leading edge blocking multi-cavity tip is applied to the radial expander VGN compared to the axial turbine rotor due to the thicker blade and non-rotating characteristics, the leakage flow from the pressure side is reduced and the efficiency can be improved.

Biography

[1] Yang, Dengfeng, et al. “A Detailed Investigation of a Variable Nozzle Turbine with Novel Forepart Rotation Guide Vane.” Proceedings of the Institution of Mechanical Engineers, Part D: Journal of Automobile Engineering, vol. 233, no. 4, pp. 994–1007, Mar 2019.

[2] Liu, Y, Yang, C, Qi, M, Zhang, H, & Zhao, B. "Shock, Leakage Flow and Wake Interactions in a Radial Turbine With Variable Guide Vanes." Proceedings of the ASME Turbo Expo 2014: Turbine Technical Conference and Exposition. Volume 2D: Turbomachinery. Düsseldorf, Germany. June 16–20, 2014.

[3] Zhou C., Hodson H., “The Tip Leakage flow of an unshrouded high Pressure Turbine blade with Tip Cooling “, ASME Paper GT2009-59637, 2009.

[4] Sjolander S. A., Cao D., “Measurements of the Flow in an Idealized Turbine Tip Gap”, ASME Paper 94-GT-74, 1994.

[5] Heyes F. J. G., Hodson H. P., “Measurement and Prediction of Tip Clearance Flow in Linear Turbine Cascades”, ASME Journal of Turbomachinery, Vol. 115, pp. 376-382, July 1993.

[6] Denton, J., and Cumpsty, N., "Loss Mechanisms in Turbo machines", Proc. IMechE, Turbomachinery—Efficiency and Improvement, Paper No. C260/87, 1987.

[7] Azad, G. S., Han, J., and Boyle, R. J., "Heat Transfer and Flow on the Squealer Tip of a Gas Turbine Blade", ASME Journal of Turbomachinery, 122(4): 725-732, October 2000.

[8] Newton, P. J., Lock, G. D., Krishnababu, S. K., Hodson, H. P., Dawes, W. N., Hannis, J., and Whitney, C., "Heat Transfer and

Aerodynamics of Turbine Blade Tips in a Linear Cascade." ASME Journal of Turbomachinery, 128(2): 300-309, April 2006.

[9] Schabowski, Z., Hodson, H., Giacche, D., Power, B., and Stokes, M. R., "Aeromechanical Optimization of a Winglet-Squealer Tip for an Axial Turbine", ASME Journal of Turbomachinery, 136(7): 071004, July 2014.

[10] Zhou, C., Hodson, H., Tibbott, I., and Stokes, M., "Effects of Winglet Geometry on the Aerodynamic Performance of Tip Leakage Flow in a Turbine Cascade" ASME Journal of Turbomachinery, 135(5): 051009, September 2013.

[11] Ameri, A. A., Steinthorsson, E., & Rigby, D. L. "Effect of squealer tip on rotor heat transfer and efficiency.", 1998.

[12] Kun Du, Zhigang Li, Jun Li, Bengt Sunden, "Influences of a multi-cavity tip on the blade tip and the over tip casing aerothermal performance in a high pressure turbine cascade", Applied Thermal Engineering, Vol. 147, pp. 347-360, 2019.

[13] Heyes F. J. G., Hodson H. P., Dailey G. M., "The Effect of Blade Tip Geometry on the Tip Leakage Flow in Axial Turbine Cascades", ASME Journal of Turbomachinery, Vol. 114, pp. 643-651, July 1992.

[14] Coull, JD, Atkins, NR, & Hodson, HP. "Winglets for Improved Aerothermal Performance of High Pressure Turbines" Proceedings of the ASME Turbo Expo 2013: Turbine Technical Conference and Exposition. Vol. 6A: Turbomachinery. San Antonio, Texas, USA. June 3-7, 2013.

[15] Shao, Ziyi, et al. "Analysis of shroud cavity leakage in a radial turbine for optimal operation in compressed air energy storage system." Journal of Engineering for Gas Turbines and Power 142.7, 2020.

[16] Tamaki, Hideaki, et al. "The effect of clearance flow of variable area nozzles on radial turbine performance." Turbo Expo: Power for Land, Sea, and Air. Vol. 43161., 2008.

[17] Chen, J., Li, L., Huang, G., & Xiang, X., "Numerical investigations of ducted fan aerodynamic performance with tip-jet." Aerospace Science and Technology, 78, 510-521., 2018

[18] Yang, Dengfeng, et al. "Design and numerical analysis of a forepart rotation vane for a variable nozzle turbine." International Journal of Turbo & Jet-Engines 36.3 pp. 233-244, 2019.

Yaras, M. I., and Sjolander, S. A., "Prediction of Tip-Leakage Losses in Axial Turbines." ASME Journal of Turbomachinery, 114(1): 204-210, January 1992.

국문 초록

익스팬더는 가스를 팽창시켜 에너지를 얻는 터보 기계로, 천연가스 운송기지에서 전기에너지를 회수하는 것과 같이 산업현장에서 다양한 목적으로 사용되고 있다. 특히 방사형 익스팬더 관련 고객의 주 요구조건은 높은 성능과 넓은 운전범위, 작은 사이즈이다. 방사형 익스팬더의 유량 제어방법은 Inlet Throttle Valve (ITV)와 Variable Geometric Nozzle (VGN) 로 분류할 수 있는데, VGN 은 ITV 와 달리 익스팬더 노즐의 각도를 조절하여 노즐 출구부 속도 방향 조절을 통해 유량을 제어한다. ITV 는 제작된 설계점에서의 공력성능은 높으나 탈설계점에서의 성능이 감소하고 이에 따라 운전 범위가 좁은 특징이 있다. 반면 VGN 은 설계점에서의 성능은 상대적으로 낮으나, 탈설계점에서의 성능저하가 작고 넓은 운전범위를 확보할 수 있다. 따라서, 고객의 요구조건 만족을 위해 VGN 의 사용이 선호된다.

그러나 노즐 각도 조절이 가능한 VGN 의 특성 상, 노즐과 캐이싱 사이의 간극이 필수적으로 존재한다. 노즐에서 이러한 팁과 허브의 간극을 통해 누설 유동이 발생하며 이는 무시할 수 없는 크기의 공력 손실을 야기한다. 방사형 익스팬더의 경우 역시 공력성능 향상 및 제품 경쟁력 향상을 위해, VGN 의 간극을 통한 누설 유동 손실을 최소화할 필요가 있다.

본 연구에서는 문헌 조사를 통해 VGN 간극이 공력 손실에 미치는 영향 및 설계요소가 미치는 영향에 대해 파악하고, 팁 간극의 누설 유동 저감을 위해 기존에 선행된 연구 사례들을 분석하고자 한다. 이후 문헌 조사를 바탕으로 기존 형상과 조건에 적용할 수 있는 설계 인자를 선정하고 CFD 유동 해석 방법을 정립한다. 설계 인자를 적용한 case study 를 진행하여, 설계 변수들이 설계점에서 VGN 공력성능에 미치는

영향을 파악하고 분석한다. 최종적으로 방사형 익스팬더의 VGN 누설 유동으로 인한 공력 손실을 최소화하는 것을 목표로 한다.

주요어 : 방사형 익스팬더, Variable Geometry Nozzle, 팁 누설 유동, 캐비티 팁, 멀티-캐비티 팁
학번 : 2020-20449